Volume XXI, 41 – No. 2, 2019, DOI: 10.35116/aa.2019.0011

DESIGN OF AN ULTRA-HIGH BYPASS RATIO FAN STAGE FOR A RESEARCH TURBOJET ENGINE

Károly BENEDA*, Bence SIPULA
Budapest University of Technology and Economics, Faculty of Transportation Engineering and Vehicle Engineering, Department of Aeronautics, Naval Architecture and Railway Vehicles
H1111 Budapest, Műegyetem rkp. 3., Hungary
**Corresponding author.* E-mail: kbeneda@vrht.bme.hu

Abstract. At the Department of Aeronautics, Naval Architecture and Railway Vehicles of Budapest University of Technology and Economics there is a versatile micro turbojet test bench based on TS-21 turbostarter engine. Besides research and developement purposes it offers a more practical study and experience for the aerospace engineering students. In this study the authors have accomplished a theoretical design of an additional fan stage to the original TS-21 engine. Based on the results of this study a decision can be made, whether the modification of the present device is worth or not. For supplementing this decision, a complex feasability study was carried out from a simple one-dimensional flow analysis through computational fluid dynamics and stress analysis of the mechanical parts. If the designed equipment will be manufactured, the resulting turbofan engine can be used to model large scale types for various research and educational purposes.

Keywords: gas turbine; turbofan; aft fan; high BPR; FEM; CFD

1. INTRODUCTION

The utilization of the turbofan engines has been increasing since its presence and it has become the most commonly employed engine in the commercial and military aviation. It has benefits, like lower fuel consumption at approximately 0.8 flight Mach number [1], which is the most widely used cruise speed of large civilian aircraft. This construction also offers reduced noise levels, the slower exhaust gases make it possible, that the turbofans are significantly quieter than the alternative engine types [2].

Due to their wide spread, there is a multitude of research fields, which are nowadays investigated, like noise [3] or pollutant emissions [4], which can also include deeper insight into the physical processes of fuel management [5,6], improving control and diagnostic system to increase service life and profitability of the power plant [7,8]. This development can serve as a basis for multiple investigation fields.

A possible classification of the turbofan engines is based on the bypass ratio (BPR) as shown in Table 1, namely the ratio of mass flow rate of the bypass stream and mass flow rate entering the core engine.

Table 1 The classification of the turbofan engines by BPR [9]

Bypass Ratio	Engine designation	Employment
0,2-3	low BPR turbofan	military engines, higher flight Mach numbers, early commercial aircraft
4-6	high BPR turbofan	usual commercial aeroplanes, military transport vehicles
8-12	ultra high BPR turbofan	recently developed engines for less fuel consumption and emission

In the specifications of the newest turbofan engines as CFM LEAP-1A or General Electric GEnx can be found some noteworthy developments of the predecessor of each. For example, as we compare the LEAP-1A and CFM's previous turbofan engine, namely the CFM56-5B, the LEAP-1A has a thrust specific fuel consumption approximately 14 percent less, than the CFM56, nevertheless it provides more thrust [9].

There is an experimental turbojet engine at the Department of Aeronautics, Naval Architecture and Railway Vehicles of Budapest University of Technology and Economics, namely the TKT-1, that has been built from a TSz-21 gas turbine. It has a single stage centrifugal compressor, annular combustion chamber and single stage axial gas generator turbine. In this study a theoretical fan design is done in connection with the TKT-1 jet engine.

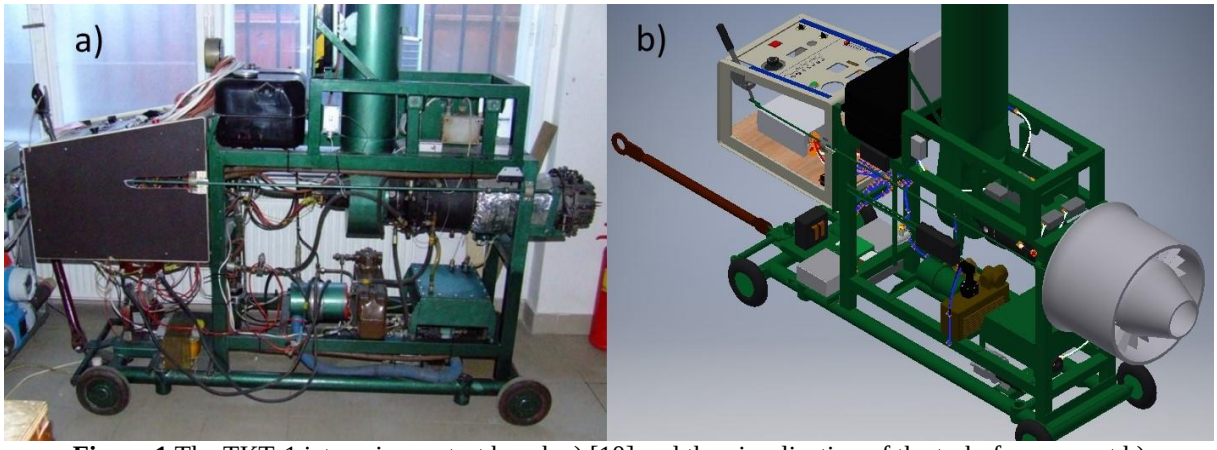

Figure 1 The TKT-1 jet engine on test bench a) [10] and the visualization of the turbofan concept b)

2. DESIGN OF THE AFT FAN STAGE

2.1 Determining the fundamental geometrical parameters

Due to the constraints of the original layout of the TS-21 engine, an aft fan could be attached with less effort in contrast to almost exclusively spread front fan used on the vast majority of aviation turbofans.

The properties of air are taken from the International Standard Atmosphere at sea level, under static conditions, as the proposed test bench could operate under such circumstances. The chosen initial parameters:

- BPR = 11 to model up-to-date engine constructions;
- Inner diameter = 0.3 m to allow enough space around the core engine;
- Velocity of the air at the inlet = 120 m/s in order to keep the Mach number in the rotating assembly at a reasonably low level.

The mass flow rate taken from the documentation of the TS-21 is 1.18 kg/s [11]. According to the definition of bypass ratio:

$$BPR = \frac{\dot{m}_{cold}}{\dot{m}_{hot}}. \tag{1}$$

From this equation the mass flow rate of the bypass stream:

$$\dot{m}_{cold} = \dot{m}_{hot} \cdot BPR = 1.18\,kg/s \cdot 11 = 12.98\,kg/s \tag{2}$$

Based on continuity the required surface is:

$$A = \frac{\dot{m}}{\rho \cdot c_1} = \frac{12.98\,{}^{kg}/_{s}}{1.225\,{}^{kg}/_{m^3} \cdot 120\,{}^{m}/_{s}} = 0.0883 m^2 \tag{3}$$

2.2 Determining the fan stage power requirement and turbine power

There were calculations made with three different bypass ratio (BPR) values and within them three pressure ratio values. The most suitable version was chosen based the graphs shown in Figure 2. The BR = 11 requires more torque, than the The BR = 7 version as seen in Figure 2 and the turbine can provide this amount at lower RPM, namely at 22200 1/min. That was considered as the most benefitical option, because the lower RPM results in less tangential velocity at the tip of blades. Furthermore there is a fairly small amount of loss of the maximal turbine power, the BR = 11 version could utilise 53 kW out of 58 kW.

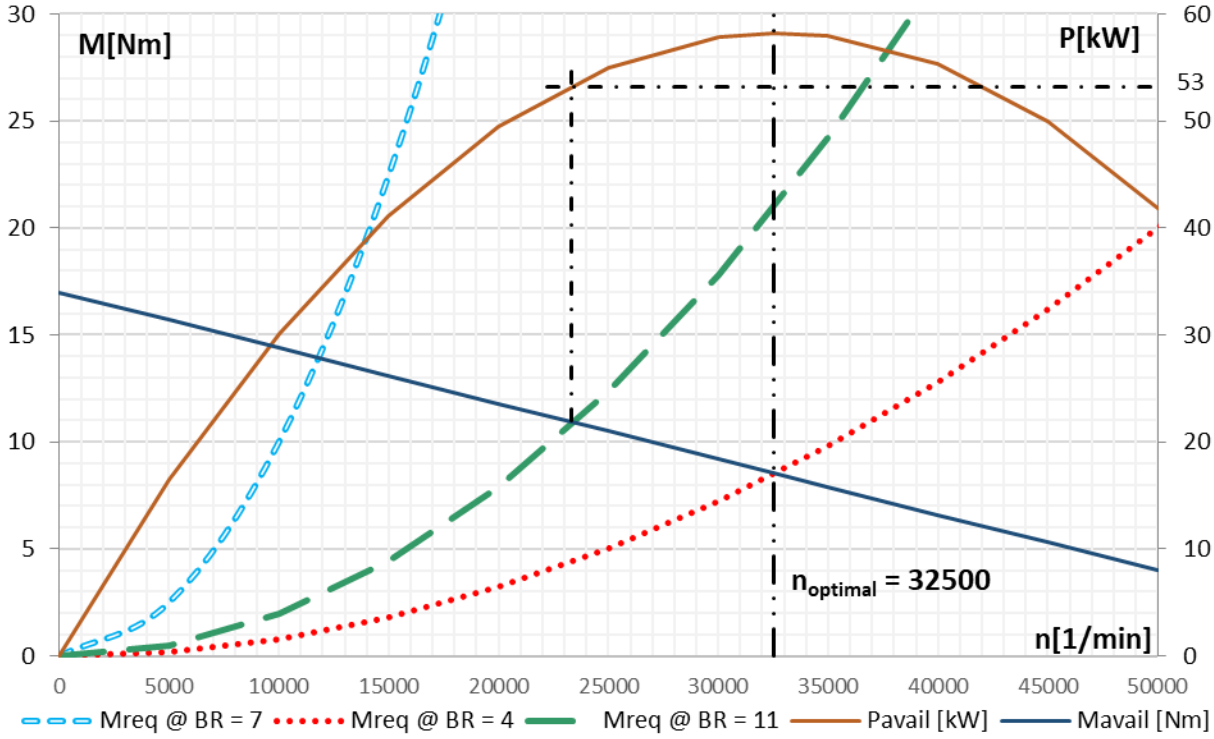

Figure 2 Turbine power characteristics and compressor power requirements at different bypass ratios

2.3 Determining the geometry of the blades of the rotor

The refined geometry of the fan blades was designed based on scientific literature [12].
The important results of the design:
The length of blades: $l = 0.085\,m$
The number of blades: $z = 18\,pcs$

Normally, the vane angles in the stator cascade should be determined in a similar way as it was carried out in the case of the rotating blades. However, as the rotor does not imply a significant flow deflection under all operational circumstances, it was not necessary to perform a detailed design. The maximum deviation from axial direction is only 8 degrees, which allows a simple straight vane to be placed downstream of the rotor. Using this concept, the geometry is significantly simplified, meanwhile the leading edge will have a small incidence at higher loads, that is still much below the

stall margin. This can be seen later in Fig. 6 where the simplified three dimensional flow domain is represented.

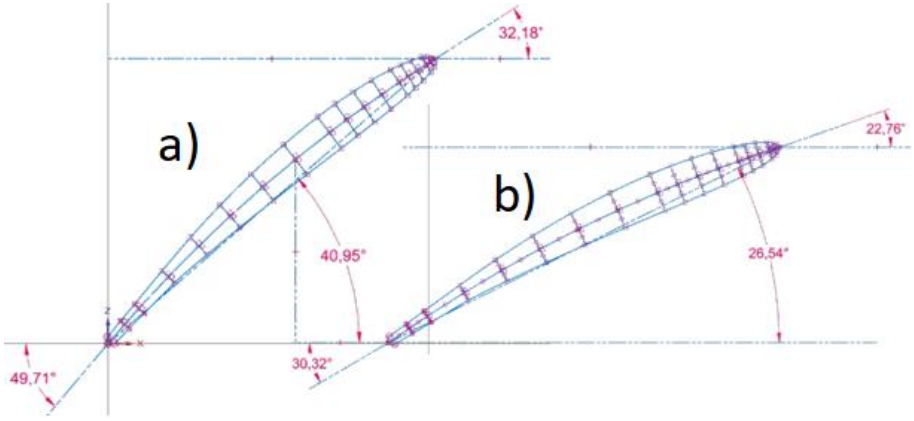

Figure 3 Sections of the rotor blade at the tip a) and at the root b)

3. STRUCTURAL ANALYS

The structural analysis was performed with the software Inventor from Autodesk. The blades were placed in the disk and they were checked as a structure. The most significant load is a result of the rotational motion. The load from the aerodynamic forces are normally about 20-30 percent of the centrifugal load, however, in this case the stage pressure ratio, consequently the blade loads are significantly less then usually. Therefore, the loads from aerodynamic forces were neglected.

The simulation was done with general aluminium alloy. The maximum value of displacement is 0.8139 mm at the tips of the blades as shown in Figure 4 and the location of the maximum stress can be found in the disk groove, where the blades are inserted, its value is 188.5 MPa as shown in Figure 5. The minimum safety factor is 1.46.

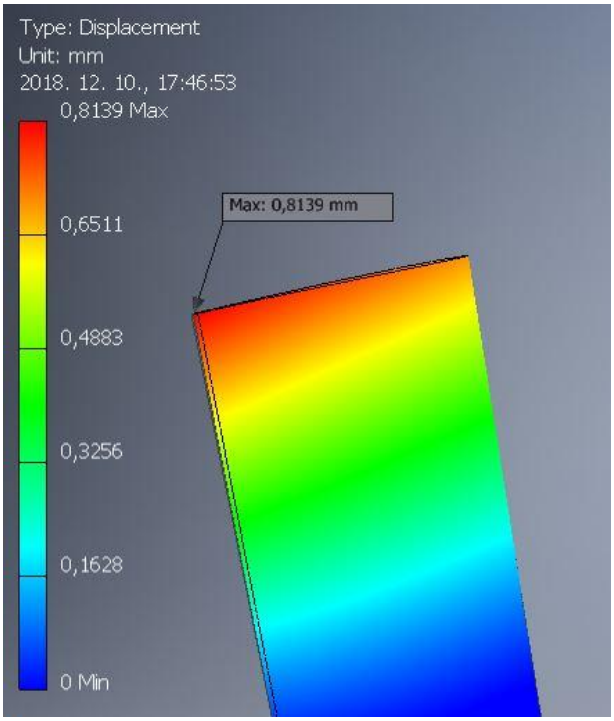

Figure 4 Displacement of the blade tip

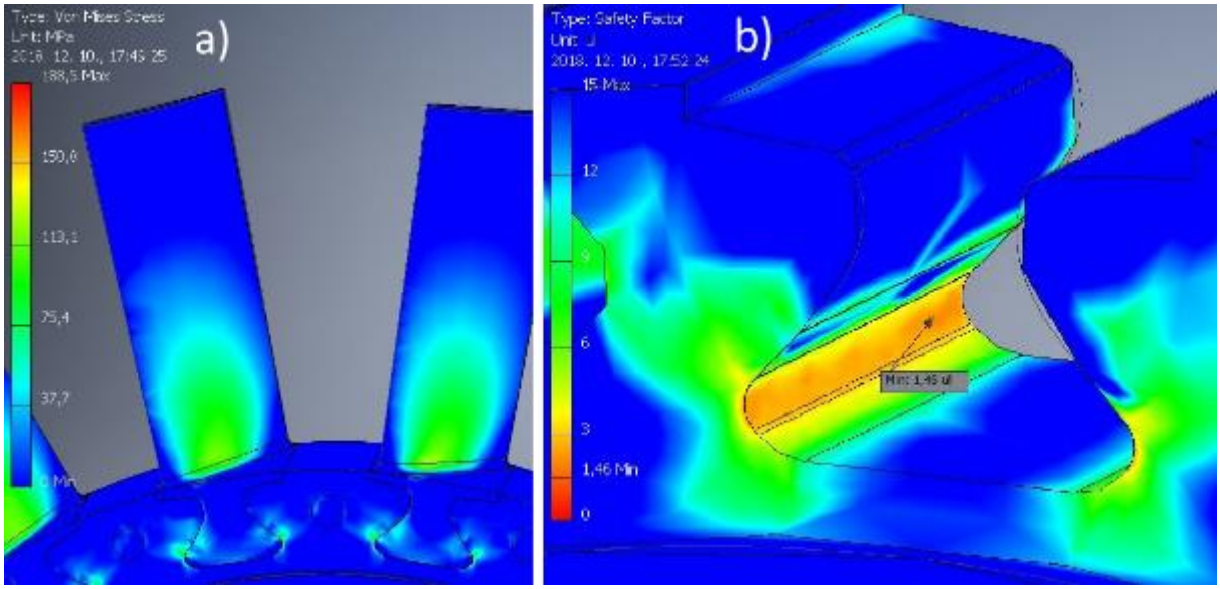

Figure 5 Location of the maximum stress: a) overview of blade and disk b) detail of disk slot

The mesh independency test was performed between 75000 and 750000 elements, and it shows, that the results have a convergence rate of 5.59 %.

4. CFD SIMULATION

The CFD simulation has been accomplished in the CFX environment of ANSYS Academic version. This allows a limited number of mesh nodes and elements, but regarding the preliminary nature of this investigation these limitations were not posing significant restriction on the results.

4.1 The flow domains

Considering the computational capacity, instead of the entire geometry only a section of the whole model was simulated, namely 3 blades in the rotor and 3 blades in the stator. That is how the flow domain was built, shown in Figure 6. The silver domain on the left is the inlet, the grey domain is the rotating cascade, followed by the stator in orange and the last green domain on the right is the outlet.

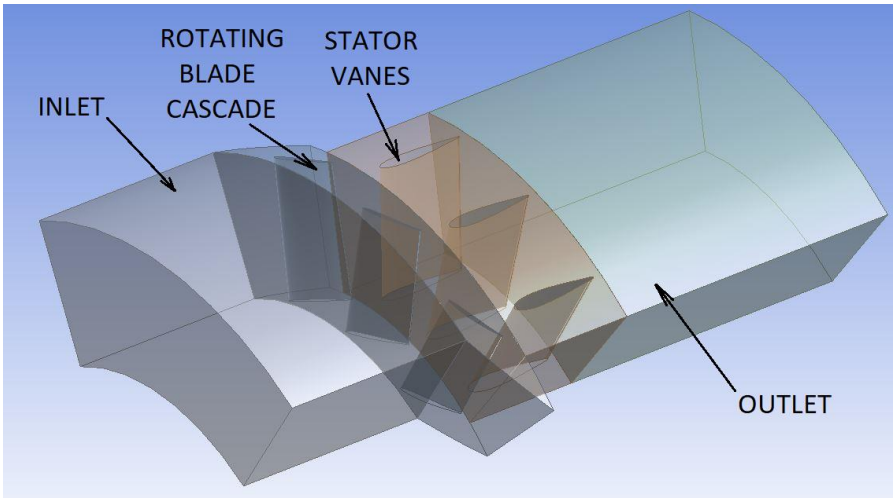

Figure 6 The different flow domains

4.2 Meshing

In the rotor and stator was the body sizing set to 4 mm, in the inlet and outlet to 6 mm. The face sizing of the rotor and stator was set to 4 and 5 mm, on the cylindrical surfaces of the inlet and outlet it was set to 5 mm. On the surfaces of the blades was set a finer meshing also, 3 mm in the rotor and 3.5 mm in the stator and the size function was set to curvature with a local minimum size of 0.25 mm.

On all of the wall surfaces there was inflation applied, all of them with the same settings. A total of seven layers, with a growth rate of 1.35 and the maximum thickness set to 1.5 mm.

With the mentioned settings the mesh of the whole domain has 796292 nodes and 2645946 elements, which is indicated in Fig. 7.

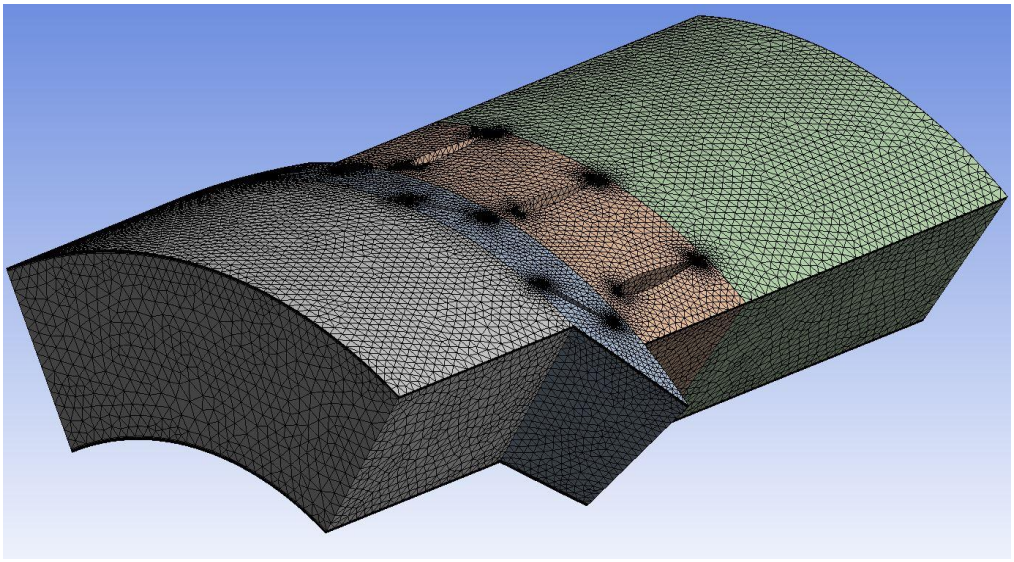

Figure 7 Meshing of the domains

4.3 Setup

Due to the reduced flow domain, rotational periodicity interfaces were set on the cut surfaces of each domain, that are shown with curved purple arrows in Figure 8. The black arrows show the direction of air flow.

Between each domain were set interfaces with general connection. On both sides of the rotor frozen rotor setting was applied and between the rotor and stator a pitch change was set. The reason behind this setting is that the stator has five more blades compared to the rotor, thus the section of this domain is of a smaller extent.

On the outer cylindrical surface of the rotor a counter rotating wall boundary was placed.

As inlet there were ambient total temperature and mass flow rate applied as shown in the following equation, where 3 is the number of modelled blades and 18 is the total blade number:

$$\dot{m} = \frac{3}{18} \cdot 12.98 \, {}^{kg}\!/_{s} = 2.166 \, {}^{kg}\!/_{s} \tag{4}$$

On the outlet was static pressure set, with the value of 1660 Pa. The simulation was done also with the difference of the boundaries on the inlet and outlet. Ambient total pressure and temperature were set on the inlet and static pressure on the outlet. The results were the same with a negligible difference.

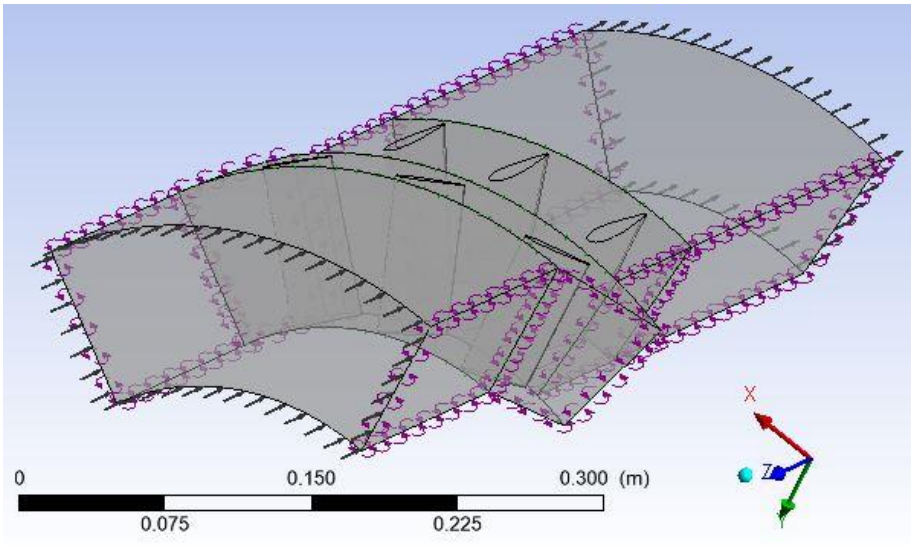

Figure 8 Boundaries on the domains

4.4 Solution

As Figure 9 shows the imbalances have converged within 200 iterations, their values are well below 1 percent, which is usually considered as a level of confidence.

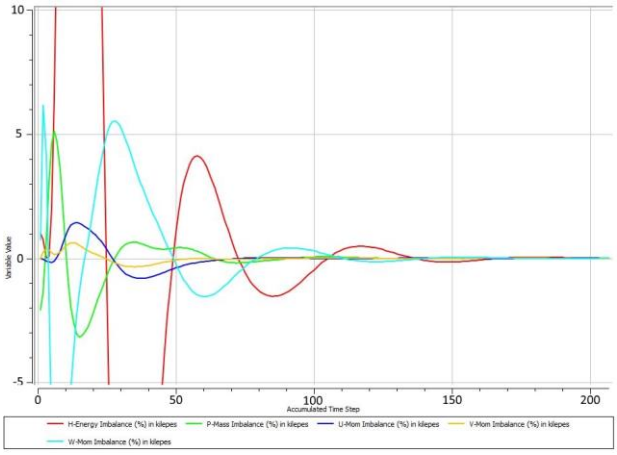

Figure 9 The values of imbalances

4.5 Results

The most of the results have minimal difference to the result of the calculations. That is caused probably by the values of efficiency, that were estimated values. There were cases, when semi-empirical formulae were used. The streamlines show the expected way of airflow. The highest value of velocity can be found on the low pressure side of the rotor blades, where the increased magnitude is due to the peripheral speed of the rotating frame.

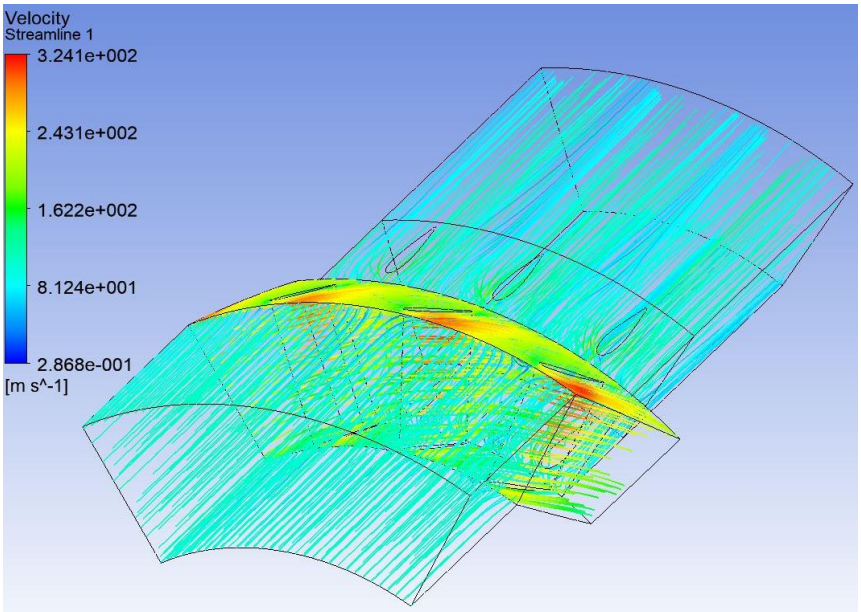

Figure 10 The streamlines through the flow domains, starting from the inlet at left

The distribution of pressure on the outlet is shown in Figure 11. The average pressure on the outlet is 108452 Pa, the result of the calculation was 106046 Pa. The difference is due to the above mentioned experimental value of the efficiency. These values have been determined for highly loaded blade cascades, however, in this case the stage pressure ratio is rather low, which probably allows higher efficiency.

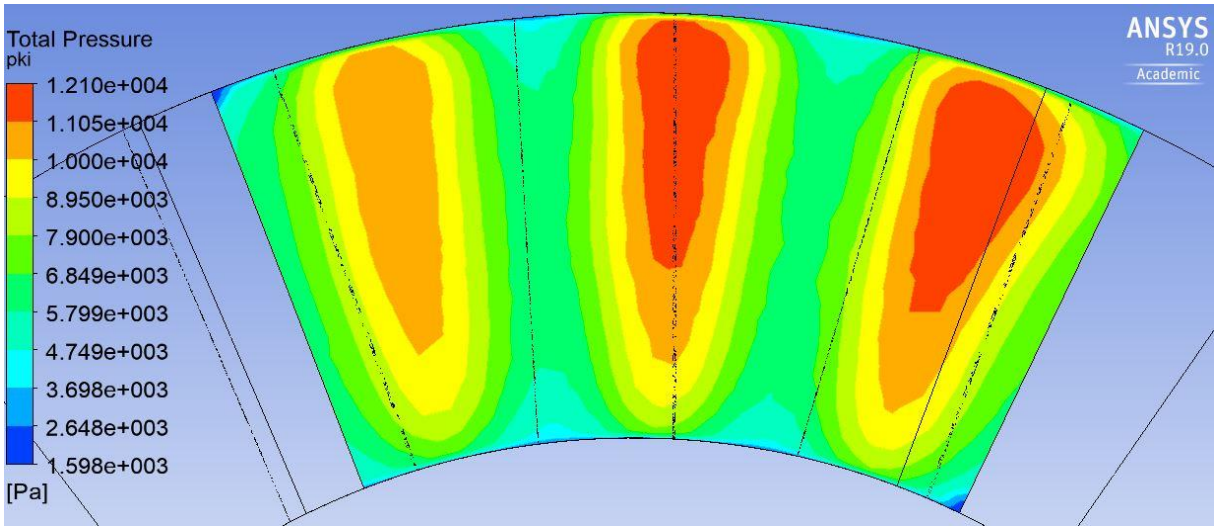

Figure 11 Distribution of total pressure on the outlet

The dimensionless wall distance y^+ is an important value of the boundary layer. In this case the maximum value of it is 53.58, but the average value is around 35 as seen in Figure 12. This variable must fall between 20 and 200, to allow an appropriate modeling of the boundary flow structure. According to the presented values one can state that the CFD simulation can be accepted as these values are corresponding to the requirement on all surfaces.

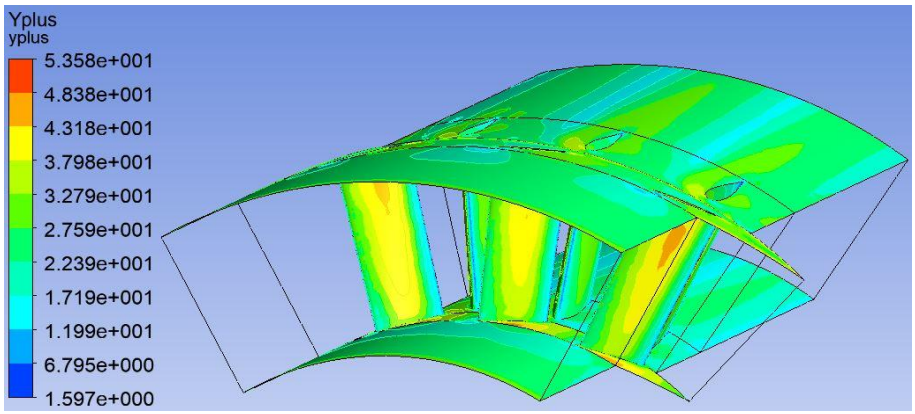

Figure 12 The values of y^+

In order to inspect the effect of the quality of meshing on the results of the simulation, a mesh independency survey has been carried out in a wide range of node numbers. As illustrated in Fig. 13, there were selected parameters whose change against node number was plotted. According to the trend of these variables one can state that the CFD results do not change significantly over 1.000.000 node number.

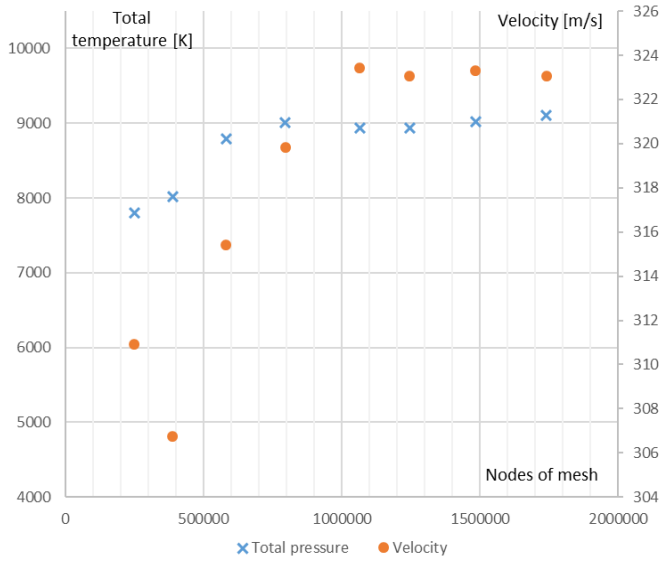

Figure 13 Values of the mesh independency test

5. CONCLUSION

The authors have performed a preliminary design of a fan stage for a micro turbine engine that could be used in research and higher education.

The first step of the design included the selection of the appropriate bypass ratio, pressure ratio, rotating speed and power requirement adapted to the available power from the free turbine of the TS-21 turbostarter. After several initial investigations with the original reduction gearbox it was clear that the power-torque curve of the turbine is not optimal for that largely reduced speed. The fan requires more peripheral speed so the reduction gearbox was considered as a next step of the design and now was set to a ratio which resulted in an optimal speed configuration for the fan stage.

During the following steps of the design two aerodynamic modelling was performed, one simplified one-dimensional and a three-dimensional CFD study. The mechanical arrangement of the fan stage was

also modelled in finite element method and the resulting stresses were compared with allowable limits applicable to general aluminium alloys that could be used as a basis for manufacturing.

The turbofan engine based on the TS-21 turbostarter could produce 1337 N thrust, which is about four times more than the TKT-1 turbojet developed from the same type. The conversion would not require much modification and new opportunities of research would occur.

As a further step of the development, before manufacturing the fan stage the reduction gearbox shall be redesigned as the authors have taken a floating output speed to optimize the fan performance, which has resulted in a much smaller reduction ratio.

Another interesting study could be the realization of a front-fan configuration that would supercharge the core engine resulting in a boost of power section performance as well.

References

[1] Klaus Hünecke. *Jet Engines – Fundamentals of Theory, Design and Operation*, Motorbooks International, 1997, p. 9-11.

[2] S. Moreau, M. Roger: Advanced noise modeling for future propulsion systems. *International Journal of Aeroacoustics*, Vol. 17, No. 6-8, pp. 576-599. https://doi.org/10.1177/1475472X18789005

[3] Samokhin, V., Moshkov, P., Yakovlev, A. Analytical Model of Engine Fan Noise. *Akustika*, 2019, Vol. 32, pp. 168-173.

[4] D.A. Block Novelo, U. Igie, V. Prakash, A. Szymański. Experimental investigation of gas turbine compressor water injection for NOx emission reductions. *Energy*, Vol. 176, pp. 235-248, doi: 10.1016/j.energy.2019.03.187

[5] Alajmi A.E.S.E.T., Adam N.M., Hairuddin A.A., Abdullah L.C. Fuelatomization in gas turbines: A review of noveltechnology. International Journal of Energy Research. 2019;43, pp. 3166–3181. https://doi.org/10.1002/er.4415

[6] P. Lokini, D. K. Roshan, A. Kushari. Influence of Swirl and Primary Zone Airflow Rate on the Emissions and Performance of a Liquid-Fueled Gas Turbine Combustor. *Journal of Energy Resources Technology*, Vol. 141, No. 6, 2019, 9 pages, doi: 10.1115/1.4042410

[7] Andoga, R., Fozo, L., Judicak, J., et. al. Intelligent Situational Control of Small Turbojet Engines. *International Journal Of Aerospace Engineering*, 2018, doi: 10.1155/2018/8328792

[8] Nyulaszi, L., Andoga, R., Butka, P., Fozo, L., Kovacs, R., Moravec, T. Fault Detection and Isolation of an Aircraft Turbojet Engine Using a Multi-Sensor Network and Multiple Model Approach. *Acta Polytechnica Hungarica*, 2018, Vol. 15, No. 2, pp. 189-209, doi: 10.12700/APH.15.1.2018.2.10

[9] Beneda, K., Főző, L.: Approximate Thermodynamic Analysis of the CFM LEAP-1A Turbofan Engine (A CFM LEAP-1A hajtómű közelítő termodinamikai analízise, in Hungarian). *Repüléstudományi közlemények*. Vol. 29, No. 2, 2018, pp. 261-274. http://www.repulestudomany.hu/folyoirat/2018_2/2018-2-22-0463- Beneda_Karoly-Ladislav_Fozo.pdf

[10] Web site of Károly Beneda, details of TKT-1 (in Hungarian), Available at: http://marert.fw.hu/tsz21/tsz21ig/tkt-1.htm

[11] Leistungsnachrechnung Starter-Triebwerk TS-21, p. 20-21.

[12] Sánta, I.. *(Segédlet gázturbinás repülőgép hajtómű évfolyamterv készítéséhez, in Hungarian)*. Budapest, 2004, p. 33-47, 65-68.

Received 06, 2019, accepted 12, 2019